longer a temperature effect on the unpinning mechanism, but there is always the amplitude-dependent effect on the attenuation dips. The inhomogeneous GQO peak does not change with the temperature up to 3°K.[12] Hence the dip-height decrease along with the ultrasonic-amplitude increase leads to the appearance of the GQO peak at 1.1°K when one increases the ultrasonic amplitude (Fig. 2).

Our study on mercury shows the high-magnetic-field effect on the electron-dislocation interaction; the same electrons which give a dislocation damping give the Landau damping of the ultrasonic wave. The typical values of the wave vector q associated with the dislocation strain field are much larger than the usual values of the ultrasonic wave vector q.[7,8] That means it will be much easier to satisfy $ql \gg 1$ (l is the electron mean free path) for dislocation damping than for Landau damping.

The author is grateful to Professor J. Friedel for valuable discussions and wishes to thank Professor W. Mercouroff, R. Reich, M. Ribault, and P. Demianozuk for their assistance.

[1]G. Bellessa, M. Ribault, and R. Reich, Phys. Lett. 31A, 556 (1970).
[2]V. L. Gurevitch, V. G. Skobov, and Yu. A. Firsov, Zh. Eksp. Teor. Fiz. 40, 786 (1961) [Sov. Phys. JETP 13, 552 (1961)].
[3]S. H. Liu and A. M. Toxen, Phys. Rev. 138, 487 (1965).
[4]E. A. Kaner and V. G. Skobov, Zh. Eksp. Teor. Fiz. 53, 375 (1967) [Sov. Phys. JETP 26, 251 (1968)].
[5]What we call low amplitude has no absolute meaning because we do not know what is lost in the transducer-crystal junction. In this particular case, there was 70 V peak to peak on a 4-mm-diam piezoelectric transducer.
[6]B. R. Tittmann and H. E. Bömmel, Phys. Rev. 151, 178 (1966).
[7]Ref. 6, Appendix.
[8]V. Ya. Kravchenko, Fiz. Tverd. Tela 8, 927 (1966) [Sov. Phys. Solid State 8, 740 (1966)].
[9]A. V. Granato and K. Lücke, in *Physical Acoustics*, edited by W. P. Mason (Academic, New York, 1966), Vol. 4A, p. 225.
[10]J. Friedel, *Dislocations* (Pergamon, New York, 1967), p. 357.
[11]A. H. Cottrell, S. C. Hunter, and F. R. N. Nabarro, Phil. Mag. 44, 1064 (1953).
[12]The inhomogeneous line does not change with temperature if $[C\Delta(x)]_{max}$ is larger than the temperature; this is our case since $[C\Delta(x)]_{max} \simeq 3$°K.
[13]We do not know the deformation amplitude necessary to break away the dislocations from impurities in mercury, but we know that in lead a deformation amplitude as small as 5×10^{-7} is sufficient to break away the dislocations from impurities [W. P. Mason, in *Physical Acoustics*, edited by W. P. Mason (Academic, New York, 1966), Vol. 4A, p. 324].

One-Electron Analysis of Optical Data in Copper

A. R. Williams, J. F. Janak, and V. L. Moruzzi
IBM Thomas J. Watson Research Center, Yorktown Heights, New York 10598
(Received 15 December 1971)

Calculations of the interband absorption $\epsilon_2(\omega)$ and the energy distribution of photoemitted electrons $D(E,\omega)$ for copper have been performed with sufficient precision to test the adequacy of the direct transition theory and the effective one-electron potential due to Chodorow. Agreement with experiment is good with no *ad hoc* adjustments and excellent when the d phase shift is increased slightly for energies above E_F. The calculations support recent experimental estimates of the L gap.

In all but the simplest models, optical data can be related to assumptions concerning the electron-electron and electron-ion interactions only by a complex computational chain consisting of many links, the most prominent and well studied of which are (1) reduction of the many-electron problem to an effective one-electron problem; (2) calculation of the band energies; (3) evaluation of the interband momentum matrix elements; (4) $\vec{k}$-space interpolation of these quantities to a mesh fine enough to permit accurate integration; and (5) evaluation of the $\vec{k}$-space integrals defining the experimental measurables. We do not deal here at all with step (1), but we have executed steps (2) through (5) with sufficient accuracy to provide a convincing test of the simple one-electron direct-transition theory of both optical absorption and photoemission and of the effective one-electron potential due to Chodorow.[1]

For both calculations described below the band

energies and interband momentum matrix elements were obtained directly from the one-electron potential at 240 $\vec{k}$'s in the irreducible $\frac{1}{48}$ of the Brillouin zone by the Koringa-Kohn-Rostoker (KKR) method.[2] A $\vec{k}\cdot\vec{p}$ Hamiltonian[3] was then constructed in each of the 240 small subvolumes surrounding the original $\vec{k}$'s, from which we then obtained the same quantities at 10 100 $\vec{k}$'s in the $\frac{1}{48}$ [the maximum distance over which $\vec{k}\cdot\vec{p}$ was used was $0.073(2\pi/a)$]. Finally, zone integrations were performed by the Gilat-Raubenheimer method with suitable generalizations.[4]

The dielectric constant.—The results of our calculation of $\epsilon_2(\omega)$, the corresponding experimental data taken by Pells and Shiga,[5] and the results of an earlier calculation by Mueller and Phillips[6] appear in Fig. 1. Since the input Chodorow potential, the underlying theoretical framework, and the objectives of the two calculations are identical, the differences between the results are due entirely to the relative accuracy with which the energies, matrix elements, etc. were evaluated. The greatest difference occurs in the vicinity of the leading edge ($\hbar\omega \sim 2$ eV) where the contributing transitions involve d states. For the corresponding momentum matrix elements, Mueller and Phillips relied on Phillips's partial-sum rules.[7] The superior agreement of our calculation with experiment in the 2-eV region therefore casts doubt on the validity of the partial-sum rules and not, as Mueller and Phillips suggest, on the underlying effective one-electron picture.

Near 4 eV both calculations display a considerable deviation from experiment. The spurious peak is due not to computational methodology but to the Chodorow potential, which misplaces the nearly free-electron–like bands near L by about 10%. Contributions to $\epsilon_2(\omega)$ from these states are virtually identical in the two calculations. Agreement with experiment is strikingly improved when the d phase shift is smoothly and slightly increased for energies above the Fermi level so as to increase the $E(L_1)$-$E(L_{2'})$ energy gap from 4.6 to 4.9 eV.[8] Results of this calculation are shown in Fig. 2 along with experimental data taken by Pells and Shiga,[5] other data taken by Nilsson,[9] and the results of an eight-parameter pseudopotential calculation by Fong *et al.*[10] Our calculation and the two experimental curves have extremely similar shapes. The uncertainty in the overall amplitude of the experimental curve probably results from different extrapolations to high photon energies of the reflectivity data required to obtain ϵ_2 by a Kramers-Kronig analysis.

In our opinion, this calculation is both somewhat more accurate and of somewhat greater fundamental significance than that of Fong *et al.* (because of the type and quantity of empirical adjustments involved), but the more important implication of Fig. 2 is the apparent adequacy of the one-electron direct-transition theory of optical absorption suggested by both calculations.

Our conclusions concerning the L_1-$L_{2'}$ gap are entirely consistent with the piezoreflectance data of Gerhardt[11] and the photoemission measurements of Lindau and Wallden.[12] Gerhardt infers from the data that the threshold for the transitions between nearly free-electron states is slightly below 4.3 eV; Lindau and Wallden put it at 4.15 eV; our adjusted calculation puts it as 4.2 eV, whereas the Chodorow potential puts it at 3.7 eV. The reason that opening up the L gap by only 0.3 eV causes such a change in the computed $\epsilon_2(\omega)$ is that, first, it causes a 0.5-eV displacement of the threshold and, second, the cubic dependence of $\epsilon_2(\omega)$ on the gap width translates the 10% shift in the gap width into a 30% change in the contribution of these states to ϵ_2. Gerhardt estimates that these states contribute 30% of the

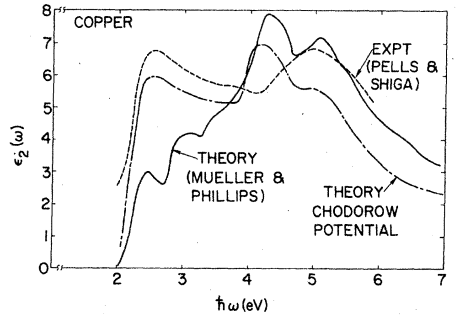

FIG. 1. Interband contribution to the imaginary part of the dielectric function as a function of photon energy.

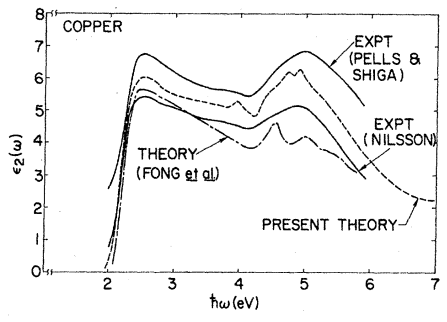

FIG. 2. Interband contribution to the imaginary part of the dielectric function as a function of photon energy.

total $\epsilon_2(\omega)$ for $\hbar\omega \sim 4$ eV; the Chodorow potential implies a fraction of 40%, while our altered phase shifts give 30%.

Photoemission.—Energy analysis of photoemitted electrons, since it provides an entire curve at each photon energy $\hbar\omega$, affords a greater opportunity for testing theories of electronic structure than $\epsilon_2(\omega)$, which is a single number at each photon energy. The price for this additional information is the increased complexity of the theory required to interpret the data; whereas for ϵ_2 it appears adequate to describe the photoexcitation process alone, for the photoemission energy distribution curve $D(E, \omega)$ it is also necessary to include the transport of the excited electrons to the crystal surface and their escape into vacuum.

The theory of photoemission is potentially very complex. It might be necessary, for example, to consider excitation, transport, and excape as a single process.[13-15] Excitation might involve more than simple direct transitions between Bloch states of the bulk.[16] It might be necessary to include the Coulomb interaction between the excited electron and the hole left behind.[17] We feel it desirable in such a situation to first determine the adequacy of the conceptually simplest theory, and have therefore implemented such a theory with sufficient internal accuracy to provide, by comparison with experiment, a measure of the importance of the more complicated effects not included.

Our basic theoretical framework is that of independent excitation, transport, and escape introduced by Berglund and Spicer.[16] We use the same semiclassical nearly free-electron description of escape used by Berglund and Spicer[16] and by Smith and Spicer.[18] Our treatment of transport is also the same as that used elsewhere, except that the electron is given the group velocity produced by the band calculation, and the mean free path due to electron-electron scattering is obtained from the computed band density of states using Kane's random-$\vec{k}$ model.[19] The excitation process is described by direct transitions between Bloch states, as in the calculation of Smith and Spicer[18]; in contrast to their work, however, our band energies and momentum matrix elements are obtained directly from the Chodorow potential via the KKR method. The zone integration is performed using Janak's generalization of the Gilat-Raubenheimer method for this problem,[4] and the spectral density of the hole states is taken to be a Lorentzian with the half-life computed from Kane's random-$\vec{k}$ model (we found the results quite insensitive to the shape of the electron spectral function).

Figure 3 shows the photoemission surface $D(E, \omega)$ implied by the Chodorow potential using the model described above. $D(E, \omega)$ is the number of electrons excited into vacuum from initial states of energy E by a photon of energy $\hbar\omega$. Two important points emerge immediately from Fig. 3(a): (i) The fact that the entire $D(E, \omega)$ surface shown in the figure is in principle experimentally accessible demonstrates the quantity of information made available by photoemission; (ii) structure which is essentially stationary in ω (particularly over the ~5-eV photon energy range scanned by the earlier experiments) frequently results from direct transitions and therefore should not be taken to imply nondirect transitions.

The left-hand portion of the photoemission surface [initial energies < -5 eV in Fig. 3(a)] is dominated by secondary electrons, i.e., those excited into conduction states by other electrons rather than by photons. This portion of the surface is generated by electron-electron scattering and is not our principal interest. The structure on the right-hand portion of the $D(E, \omega)$ surface and its ω dependence is our main interest here.

A comparison at our calculated $D(E, \omega)$ with experimental data taken by Eastman and Cashion[20] at four specific ω's is shown in Fig. 3(b). The remarkable agreement for 16.8-eV photons suggests that no theoretical complications beyond those included here are required to interpret the data. While the agreement at the other frequencies in Fig. 3(b) is not as good as it is at 16.8 eV, the theory and experiment demonstrate a very similar ω dependence; as ω is increased above 16.8 eV, both theory and experiment show a new peak growing where at 16.8 eV there was a valley —the theoretical peak appears merely to be growing faster. Similarly, the leading edge of the experimental data appears to soften at $\hbar\omega = 26.9$ eV, while theoretically this softening occurs at lower ω, and by 26.9 eV the leading edge of the theoretical curve has already shifted to the left. (We should point out that although the leading edge at 26.9 eV is displaced from the experiment by ~0.7 eV, this represents only a 3% error.) A relatively good match is obtained if one compares the experimental distributions at 21.2 and 26.9 eV with the theoretical distributions at 18.4 and 21.1 eV, respectively. The photoemission distributions implied by the Chodorow potential, in other words, appear to have approximate-

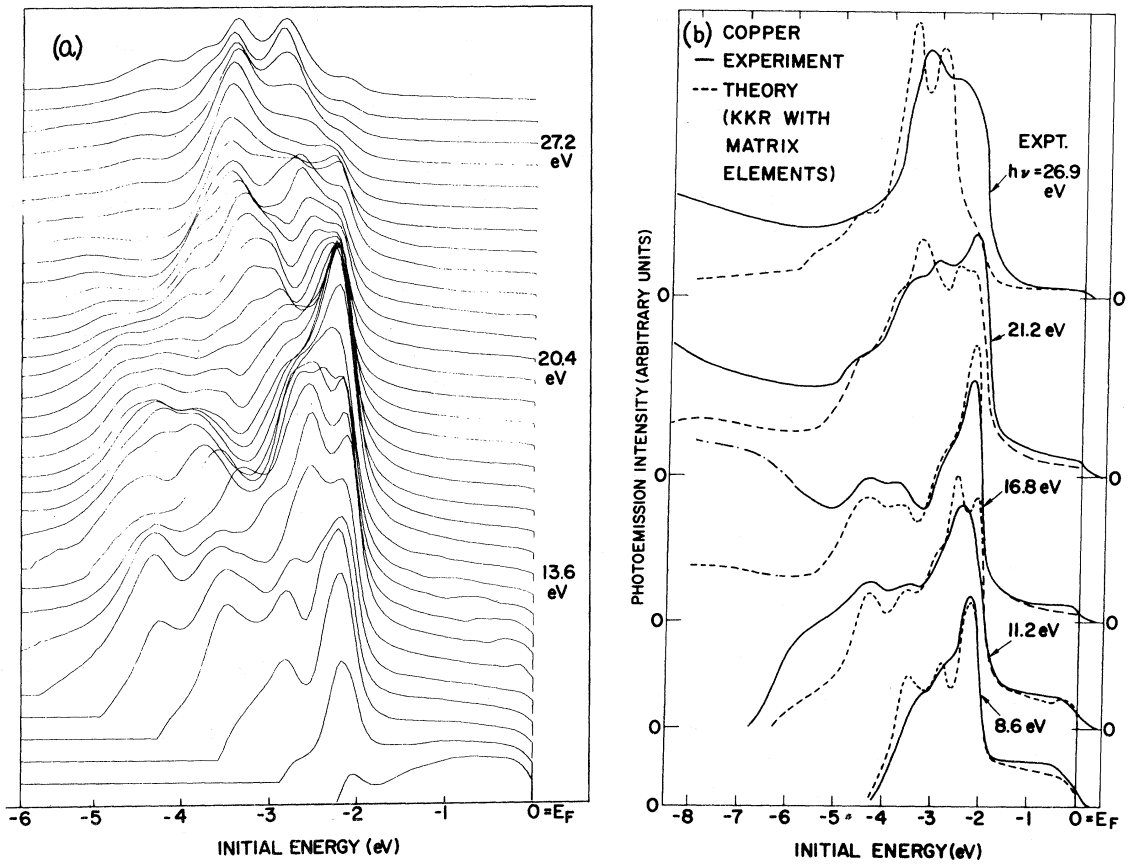

FIG. 3. (a) Theoretical photoemission surface $D(E,\omega)$ for copper as given by the Chodorow potential and direct transitions; (b) comparison with experiment.

ly the correct shape as functions of initial energy, but this shape changes too rapidly with photon energy above photon energies of 16.8 eV.

The correct ω dependence occurring at the wrong ω is just what one would expect from errors in the underlying band energies. Since our ϵ_2 calculation also calls for improved conduction-band energies, the two calculations taken together strongly suggest that the principal source of remaining theoretical-experimental discrepancies is the one-electron potential, and not the more complicated processes (vertex corrections, nondirect transitions, coupling of excitation, transport, and escape, etc.) not present in our theory.

We wish to thank Dean Eastman for his informed advice and enthusiasm.

*Based in part on work sponsored by the U. S. Air Force Office of Scientific Research, Office of Aerospace Research, under Contract No. F44620-70-0089.

[1]M. I. Chodorow, Ph. D. thesis, Massachusetts Institute of Technology, 1939 (unpublished).

[2]J. Korringa, Physica (Utrecht) 13, 392 (1947); W. Kohn and N. Rostoker, Phys. Rev. 94, 1111 (1954).

[3]M. Cardona and F. Pollak, Phys. Rev. 142, 530 (1966).

[4]J. F. Janak, in *Computational Methods in Band Theory*, edited by P. M. Marcus, J. F. Janak, and A. R. Williams (Plenum, New York, 1971), p. 323.

[5]G. P. Pells and M. Shiga, J. Phys. C: Proc. Phys. Soc., London 2, 1835 (1969).

[6]F. M. Mueller and J. C. Phillips, Phys. Rev. 157, 600 (1967).

[7]J. C. Phillips, Phys. Rev. 153, 669 (1967).

[8]The phase shifts below the Fermi energy were left unchanged, so that all ground-state properties, such as the charge density, the Fermi surface, etc., are the same as for the Chodorow potential.

[9]P. O. Nilsson, Phys. Kondens. Mater. 11, 1 (1970).

[10]C. Y. Fong, M. L. Cohen, R. R. L. Zucca, J. Stokes, and Y. R. Shen, Phys. Rev. Lett. 25, 1486 (1970).

[11]U. Gerhardt, Phys. Rev. 172, 651 (1968).

[12]I. Lindau and L. Wallden, Solid State Comm. 9, 1147 (1971).

[13]N. W. Ashcroft and W. L. Schaich, in "Electronic Density of States," edited by L. H. Bennett, National

Bureau of Standards Special Publication No. 323 (U. S. GPO, Washington, D. C., to be published).
[14]G. D. Mahan, Phys. Rev. B 2, 4334 (1970).
[15]D. C. Langreth, Phys. Rev. B 3, 3120 (1971).
[16]C. N. Berglund and W. E. Spicer, Phys. Rev. 136, A1030, A1044 (1964).
[17]S. Doniach, Phys. Rev. B 2, 3898 (1970).
[18]N. V. Smith and W. E. Spicer, Opt. Commun. 1, 157 (1969).
[19]E. O. Kane, Phys. Rev. 159, 624 (1967).
[20]D. E. Eastman and J. K. Cashion, Phys. Rev. Lett. 24, 310 (1970).

Scaling Approach to Tricritical Phase Transitions

Eberhard K. Riedel
Department of Physics, Duke University, Durham, North Carolina 27706
(Received 26 January 1972)

Scaling laws for multicomponent systems near the tricritical point are derived by relating the "scales" of the competing second-order and tricritical phase transitions. The approach leads to a consistent description of the thermodynamics of the superfluid and phase-separation transitions in He^3-He^4 mixtures.

A scaling theory is presented for multicomponent systems near the tricritical point. Crossover effects are obtained due to the competition between the second-order and tricritical phase transitions. Exponent relations are found for the scaling indices of nonordering fields and densities. A set of values is conjectured for the tricritical exponents including the crossover exponent φ_t. The scaling structure of the phase diagram is also discussed. The results will be obtained by generalizing a parameter scaling theory, derived elsewhere for anisotropic magnetic systems,[1] to the tricritical instability.

We formulate the scaling approach to multicomponent systems in terms of pairs of conjugate thermodynamic variables: entropy density s and temperature T, ordering density m and ordering field h, and nonordering density n and nonordering field g. We choose the fields as independent variables and define the densities as field derivatives of a thermodynamic potential F.[2] For liquid He^3-He^4 mixtures, for example, m corresponds to the superfluid order parameter, n to the He^3 concentration in the system, and g to the difference between the chemical potentials of the He^3 and He^4 components. In this case the ordering field h is experimentally not accesible. (Similar definitions can be made for systems exhibiting metamagnetic-antiferromagnetic transitions, etc.) A schematic tricritical phase diagram is shown in Fig. 1. At the tricritical point the system is unstable both to fluctuations in the ordering density m and the nonordering density n. This fact has been simulated by using Ising models with two competing interactions.[3,4] These models exhibit both a first-order and a second-order phase transition in analogy to the experimental situation near tricritical points.[5-7]

Along the critical line $T_c(g)$ in region II of Fig. 1 the nonordering field g does not change the second-order character of the transition. Then the universality hypothesis suggests that the thermodynamic potential has the form $F(T,g) = F_0(d_c(T, g)) + F_{\text{regular}}(T,g)$. Here F_0 is the singular part of the potential in the absence of the field g, and d_c is the effective departure of a point (T, g) from

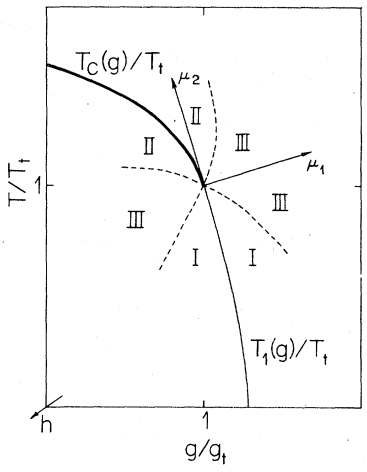

FIG. 1. Schematic phase diagram near the tricritical point (T_t, g_t) in the $h=0$ plane. The line labeled $T_c(g)$ is the line of second-order transition, and $T_1(g)$ is the line of first-order transitions. The regions of different critical behavior denoted by I to III are the first-order, second-order, and tricritical regions. The dashed curves are the crossover lines. The scaling fields are indicated by the axes μ_1 and μ_2.